



1 **Uncertain Henry's Law Constants Compromise Equilibrium**

2 **Partitioning Calculations of Atmospheric Oxidation Products**

3 Chen Wang¹, Tiange Yuan¹, Stephen A. Wood¹, Kai-Uwe Goss^{2,3}, Jingyi Li,^{4,5} Qi Ying⁴, Frank
4 Wania^{1*}

5 ¹*Department of Physical and Environmental Sciences, University of Toronto Scarborough, 1265*
6 *Military Trail, Toronto, ON, M1C 1A4, Canada*

7 ²*Department of Analytical Environmental Chemistry, Centre for Environmental Research UFZ*
8 *Leipzig-Halle, Permoserstraße 15, Leipzig, D-04318, Germany*

9 ³*Institute of Chemistry, University of Halle-Wittenberg, Kurt-Mothes-Straße 2, Halle, D-06120,*
10 *Germany*

11 ⁴*Environmental and Water Resources Division, Zachry Department of Civil Engineering, Texas*
12 *A&M University College Station, TX 77843-3136*

13 ⁵*Current Address: School of Environmental Science and Engineering, Nanjing University of*
14 *Information Science & Technology, 219 Ningliu Road, Nanjing 210044, China*

15 *Corresponding author: frank.wania@utoronto.ca, +1-416-287-7225



16 Abstract

17 Gas-particle partitioning governs the distribution, removal and transport of organic compounds
18 in the atmosphere and the formation of secondary organic aerosol. The large variety of
19 atmospheric species and their wide range of properties make predicting this partitioning
20 equilibrium challenging. Here we expand on earlier work and predict gas-organic and gas-
21 aqueous phase partitioning coefficients for 3414 atmospherically relevant molecules using
22 COSMOtherm, SPARC and poly-parameter linear free energy relationships. The Master
23 Chemical Mechanism generated the structures by oxidizing primary emitted volatile organic
24 compounds. Predictions for gas-organic phase partitioning coefficients ($K_{W/O/M/G}$) by different
25 methods are on average within one order of magnitude of each other, irrespective of the
26 numbers of functional groups, except for predictions by COSMOtherm and SPARC for
27 compounds with more than three functional groups, which have a slightly higher discrepancy.
28 Discrepancies between predictions of gas-aqueous partitioning ($K_{W/G}$) are much larger and
29 increase with the number of functional groups in the molecule. In particular, COSMOtherm
30 often predicts much lower $K_{W/G}$ for highly functionalized compounds than the other methods.
31 While the quantum-chemistry based COSMOtherm accounts for the influence of intramolecular
32 interactions on conformation, highly functionalized molecules likely fall outside of the
33 applicability domain of the other techniques, which at least in part rely on empirical data for
34 calibration. Further analysis suggests that atmospheric phase distribution calculations are
35 sensitive to the partitioning coefficient estimation method, in particular to the estimated value
36 of $K_{W/G}$. The large uncertainty in $K_{W/G}$ predictions for highly functionalized organic compounds
37 needs to be resolved to improve the quantitative treatment of SOA formation.



38 Introduction

39 Volatile organic compounds (VOCs) emitted to the atmosphere are oxidized to form secondary
40 products. These products tend to be more oxygenated, less volatile and more water-soluble
41 than their parent compounds, and thus have higher affinity for aerosol particles and aqueous
42 droplets. Equilibrium partitioning coefficients are often needed to assess the distribution of
43 these oxidized compounds among different phases in the atmosphere such as aerosol particles,
44 fog and cloud droplets. In particular, the partitioning between gas and organic phase and
45 between gas and aqueous phase is required for the evaluation of an organic compound's
46 contribution to secondary organic aerosol (SOA) formation, its transport, removal and lifetime.
47 Experimentally determined partitioning coefficients are rarely available for the oxidation
48 products of VOCs due to the difficulties in making the measurements and obtaining chemical
49 standards. Furthermore, the number of organic species in the atmosphere is in the hundreds of
50 thousands, if not higher. Their gas-particle partitioning is therefore usually predicted. Reliable
51 estimation methods for gas-organic and gas-aqueous partitioning should be applicable to a
52 wide range of organic compounds, especially to multifunctional species generated during the
53 multi-step atmospheric oxidation of precursor VOCs.

54 Current approaches for predicting partitioning into non-aqueous organic aerosol phases almost
55 exclusively rely on predictions of vapor pressure. These predictions have large uncertainties;
56 comparison among different vapor pressure prediction methods suggest increasing
57 discrepancies with increasing numbers of functional groups in an organic compound (Valorso et
58 al., 2011; Barley and McFiggans, 2010; McFiggans et al., 2010). This uncertainty matters, because
59 it is the multi-functional oxidation products that can occur in either gas or condensed phases in
60 the atmosphere. Instead of relying on predictions for vapor pressures, Wania et al. (2014)
61 proposed using three alternative methods for direct gas-particle partitioning prediction: poly-
62 parameter linear free energy relationships (ppLFRs), the on-line calculator of SPARC Performs
63 Automated Reasoning in Chemistry (SPARC) and the quantum-chemistry based program
64 COSMOtherm. Wania et al. (2014) found that partitioning coefficients predicted for the
65 oxidation products of n-alkanes are within one order of magnitude, and mutual agreement



66 does not deteriorate with increasing number of functional groups. Because of the relatively
67 small number of oxidation products in that study, the reliability of these prediction methods for
68 other organic compounds requires further evaluation.

69 While more experimental data exist for the Henry's law constant of atmospherically relevant
70 compounds than gas-organic phase partitioning coefficients (Sander, 2015), data are not usually
71 available for VOC oxidation products, which potentially have a higher affinity for atmospheric
72 aqueous phases. Currently available prediction methods for the air-water partitioning
73 coefficient include GROup contribution Method for Henry's law Estimate (GROMHE) (Raventos-
74 Duran et al., 2010), SPARC (Hilal et al., 2008), HENRYWIN in EPI suite (US EPA, 2012), and
75 ppLFRs (Goss, 2006). Sander (2015) provides a more comprehensive list of websites as well as
76 quantitative structure-property relationships for Henry's law constants. Hodzic et al. (2014)
77 developed a method to predict Henry's law constant from a molecule's volatility to be
78 implemented in atmospheric models. COSMOtherm can also predict gas-aqueous phase
79 partitioning of organic compounds, including VOC oxidation products (Wania et al., 2015).
80 Though many different methods are available for Henry's law constant prediction, they have
81 not been systematically evaluated for a large set of organic compounds of atmospheric
82 relevance. An exception is the comparison of GROMHE, SPARC and HENRYWIN predictions for
83 488 organic compounds bearing functional groups of atmospheric relevance (Raventos-Duran
84 et al., 2010).

85 The objective of this paper was to compare and evaluate gas-particle partitioning predictions
86 for a large number of organic compounds of atmospheric interest using ppLFR (in combination
87 with ABSOLV-predicted solute descriptors), SPARC and COSMOtherm. While all three methods
88 are able to estimate both gas-organic and gas-aqueous partitioning, they are based on different
89 principles: ppLFRs are empirically calibrated multiple linear regressions, SPARC contains
90 solvation models based on fundamental chemical structure theory (Hilal et al., 2004), and
91 COSMOtherm combines quantum chemistry with statistical thermodynamics (Klamt and Eckert,
92 2000). This study thus expands earlier work (Wania et al., 2014) to a much larger number of



93 compounds and to aqueous phase partitioning. As such, it includes quantum-chemistry based
94 predictions for an unprecedented number of atmospherically relevant compounds.

95 Method

96 The Master Chemical Mechanism (MCM v3.2, <http://mcm.leeds.ac.uk/MCM>) a near-explicit
97 chemical mechanism, was used to generate 3414 non-radical species through the multi-step gas
98 phase oxidation of 143 parent VOCs (methane + 142 non-methane VOCs). Reactions of the
99 parent VOCs with O₃, OH and NO₃ are included in the MCM mechanism whenever such
100 reactions are possible. The details about the studied compounds are given in the supporting
101 information (Excel spreadsheet), including the compounds' MCM ID, SMILES, precursors (i.e.
102 the parent VOC), molecular weight, molecular formula, elements, generation of oxidation,
103 number and species of functional groups, O:C ratio, and average carbon oxidation state (\overline{OS}_C)
104 (Kroll et al., 2011).

105 Three prediction methods are used to estimate the equilibrium partitioning coefficients
106 between a water-insoluble organic matter phase (WIOM) and the gas phase ($K_{WIOM/G}$) at 15 °C in
107 unit of m³ (air)/m³ (WIOM) as well as the equilibrium partitioning coefficients between water
108 and gas phase ($K_{W/G}$) at 15 °C in unit of m³ (air)/m³ (water). The two partitioning coefficients are
109 defined as:

$$110 \quad K_{WIOM/G} = C_{WIOM}/C_G \quad (1)$$

$$111 \quad K_{W/G} = C_W/C_G \quad (2)$$

112 C_{WIOM} , C_W and C_G (mol/m³) are equilibrium concentrations of an organic compound in WIOM,
113 water, and gas phase, respectively. Partitioning between gas and aqueous phase can be
114 significantly influenced by the presence of inorganic salts (i.e. the salt effect) (Endo et al.,
115 2012; Wang et al., 2016; Wang et al., 2014; Waxman et al., 2015), the hydration of carbonyls (Ip
116 et al., 2009) and the dissociation of organic acids (Mouchel-Vallon et al., 2013), particularly in
117 the aqueous phase of aerosols. However, in this study only the partitioning between gas and
118 pure water, i.e. the Henry's law constant, is predicted, and no hydration, salt effect or acid



119 dissociation is considered. Conversion of partitioning coefficients $K_{W/G}$ to Henry's constant (K_H)
120 in unit M/atm or $K_{WIOM/G}$ to saturation concentration (C^* , $\mu\text{g}/\text{m}^3$) is provided in the supporting
121 information.

122 Wania et al. (2014) describe each prediction method in detail. In brief, pPLFER-based
123 predictions rely on solute descriptors for the 3414 compounds generated with ABSOLV
124 (ACD/Labs, Advanced Chemistry Development, Inc., Toronto, Canada) as well as system
125 parameters for water-air partitioning from Goss (2006) and organic aerosol-air partitioning
126 from Arp et al. (2008). As described in Wania et al. (2014), the latter is the average $K_{WIOM/G}$
127 predicted for four different organic aerosols. For the calculations of $K_{WIOM/G}$ by SPARC and
128 COSMOtherm, the phase WIOM is represented by the surrogate structure "B" as proposed by
129 Kalberer et al. (2004) and adopted previously by Arp and Goss (2009) and Wania et al. (2014).
130 SPARC calculations were carried out using the on-line calculator ([http://archemcalc.com/sparc-](http://archemcalc.com/sparc-web/calc)
131 [web/calc](http://archemcalc.com/sparc-web/calc)), with SMILES (simplified molecular-input line-entry system) strings as input.
132 COSMOtherm predicts a large variety of properties based on COSMO-RS (conductor-like
133 screening model for real solvents) theory, which uses quantum-chemical calculations and
134 statistical thermodynamics (Klamt and Eckert, 2000;Klamt, 2005). First, TURBOMOLE (version
135 6.6, 2014, University of Karlsruhe & Forschungszentrum Karlsruhe GmbH, 1989–2007,
136 TURBOMOLE GmbH, since 2007 available from www.turbomole.com) optimizes the geometry
137 of the molecules of interest at the BP-TZVP level. COSMOconf (version 3.0, COSMOlogic) then
138 selects a maximum of ten lowest energy conformers for each calculated molecule and
139 generates COSMO files. Calculations with TURBOMOLE and COSMOconf were performed on the
140 General Purpose Cluster (GPC) supercomputer at the SciNet HPC Consortium at University of
141 Toronto (Loken et al., 2010). Finally, COSMOtherm (version C30_1501 with BP_TZVP_C30_1501
142 parameterization, COSMOlogic GmbH & Co. KG, Leverkusen, Germany, 2015) calculates
143 partitioning coefficients from the selected COSMO files at 15 °C.

144 In order to compare different predictions numerically, we calculated the mean difference (MD)
145 and the mean absolute difference (MAD) for each pair of $K_{WIOM/G}$ or $K_{W/G}$ sets:

$$146 \quad MD_{XY} = \frac{1}{n} \sum_i (\log_{10} K_{i,CP/GX} - \log_{10} K_{i,CP/GY}) \quad (3)$$



$$147 \quad \text{MAD}_{XY} = \frac{1}{n} \sum_i \left| \log_{10} K_{i,CP/GX} - \log_{10} K_{i,CP/GY} \right| \quad (4)$$

148 where CP (“condensed phase”) stands for either WIOM or water and X and Y represents two
149 prediction techniques.

150 Results

151 The Range of Estimated Partitioning Coefficients

152 Partitioning coefficients predicted for each compound with different methods are given in an
153 Excel spreadsheet as Supporting Information. All three methods predicted the $\log K_{WIOM/G}$ for
154 these organic compounds to range from approximately 0 to 15 (Figure 1 (a)-(c)). Hodzic et al.
155 (2014) predicted a $\log C^*$ in the range of -8~12 (at 25 °C) for oxidation products of different
156 VOCs (including n-alkanes, benzene, toluene, xylene, isoprene and terpenes), corresponding to
157 a $\log K_{WIOM/G}$ range of approximately 0 and 20 (see conversion in Supporting information), i.e.
158 their data set included higher $K_{WIOM/G}$ values than those generated here, even though $K_{WIOM/G}$
159 value are lower at higher temperature.

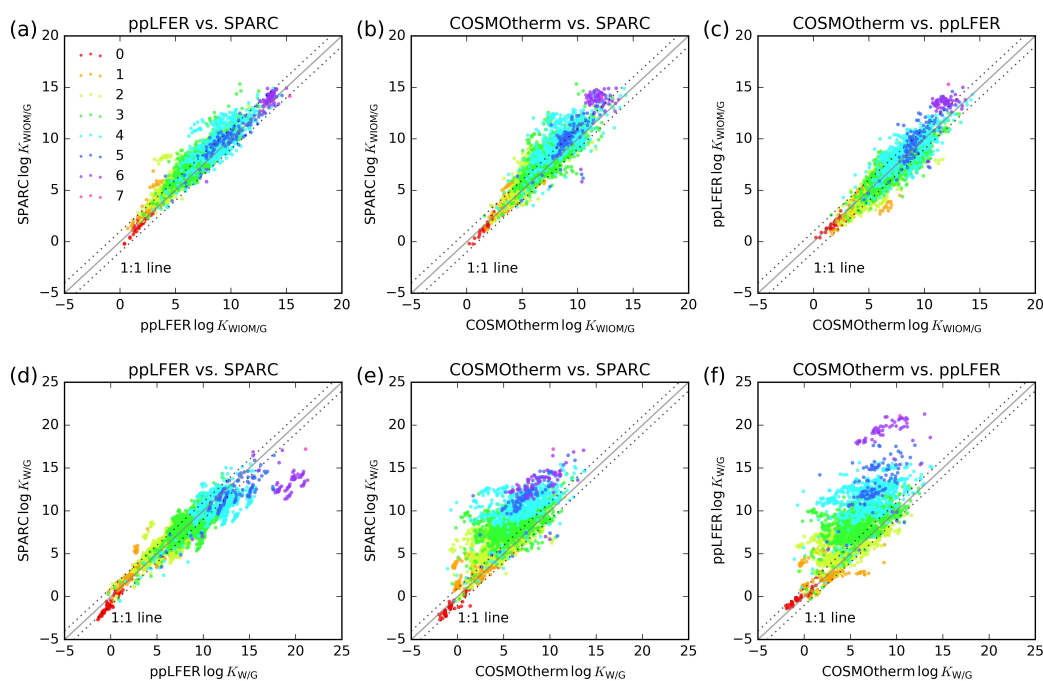
160 The $\log K_{W/G}$ range predicted for the studied compounds by the three methods is more variable
161 (Figure 1 (d)-(f)), with the ABSOLV/ppLFER predictions covering a wider range (-1.4 to 21.3) than
162 either SPARC (-2.7 to 17.2) or COSMOtherm (-2 to 13.8). Hodzic et al. (2014) predicted a $\log K_H$
163 (at 25°C in M/atm) in the range of -4 and 16 (at 25 °C), corresponding to $\log K_{W/G}$ between -2.6
164 and 17.4. The wider range of the ABSOLV/ppLFER predictions is due to much higher predicted
165 $K_{W/G}$ -values for compounds with the highest affinity for the aqueous phase.

166 Comparison between Different Prediction Methods

167 The discrepancies between different predictions (MAD and MD) are given in Table 1. The
168 agreement between the $K_{WIOM/G}$ predictions by COSMOtherm, SPARC and ABSOLV/ppLFER was
169 reasonable (Figure 1 (a)-(c)). In particular, the MAD between $K_{WIOM/G}$ predictions is less than 1
170 log units (Table 1) and therefore similar to what had been previously found for a much smaller
171 set of *n*-alkane oxidation products (Wania et al., 2014). The $K_{WIOM/G}$ -values predicted by SPARC
172 tend to be higher than those predicted by COSMOtherm and ABSOLV/ppLFER (MD of -0.64 and



173 -0.79 in log units, respectively), whereas the latter two predictions have a slightly better
174 agreement, with a MD of 0.15 log units (Figure 1 (c) and Table 1). Overall, the agreement in the
175 $K_{WIO/M/G}$ predicted with these three methods, which are based on very different theoretical
176 foundations, is much better than that between different vapor pressure estimation methods
177 commonly used for gas-particle partitioning calculations (Valorso et al., 2011).



178

179 **Figure 1** Comparison of the $K_{WIO/M/G}$ (upper panel) and $K_{W/G}$ (lower panel) predicted using
180 COSMOtherm, SPARC and ABSOLV/ppLFERs. The differently colored dots indicate the
181 number of functional groups in the molecules. The solid line indicates a 1:1 agreement.
182 The dotted lines indicate a deviation by ± 1 log unit.

183 The $K_{W/G}$ predicted by ABSOLV/ppLFEr and SPARC differ from COSMOtherm predictions
184 substantially, on average by more than two orders of magnitude. In Figure 1 (e) and (f),
185 predictions are more scattered (indicating a larger MAD) and most markers are located above
186 the 1:1 line, indicating that $K_{W/G}$ predicted by COSMOtherm are mostly lower than those
187 predicted by SPARC and ABSOLV/ppLFEr, with a MD of -2.06 and -2.42 log units, respectively.



188 These discrepancies tend to increase with the $K_{W/G}$. Raventos-Duran et al. (2010) also showed
 189 that the reliability of $K_{W/G}$ estimates made by GROMHE, SPARC and HENRYWIN decreases with
 190 increasing affinity for the aqueous phase. $K_{W/G}$ predictions by SPARC and ABSOLV/ppLFEr are
 191 more consistent (with a MAD around 1 log units, see Figure 1 (d)). The largest discrepancies
 192 between ABSOLV/ppLFEr and SPARC (and also between ABSOLV/ppLFEr and COSMOtherm)
 193 occur for compounds with the highest $K_{W/G}$ as predicted by ABSOLV/ppLFEr (purple markers in
 194 Figure 1 (d) and (f)). Further analysis indicates that these compounds have the largest number
 195 of functional groups (≥ 6) and oxygen (9~12 oxygen) in the molecule; this will be discussed in
 196 detail below.

197 **Table 1** Mean absolute differences (MAD) and mean differences (MD) between SPARC,
 198 ABSOLV/ppLFEr and COSMOtherm predictions for compounds with different numbers
 199 of functional groups

Number of Functional Groups			0	1	2	3	4	5	>5	All
Number of Compounds			63	372	1179	1064	565	111	60	3414
log $K_{W/O\&M/G}$	ppLFEr vs. SPARC	MAD	0.24	0.70	0.95	0.93	1.08	0.75	0.54	0.91
		MD	0.05	-0.70	-0.91	-0.81	-0.83	-0.24	-0.30	-0.79
	COSMOtherm vs. SPARC	MAD	0.36	0.48	0.80	0.94	1.42	1.22	2.11	0.94
		MD	0.29	-0.19	-0.55	-0.57	-1.21	-0.78	-1.83	-0.64
	COSMOtherm vs. ppLFEr	MAD	0.32	0.67	0.63	0.74	0.89	0.93	1.72	0.73
		MD	0.24	0.51	0.36	0.24	-0.38	-0.54	-1.53	0.15
log $K_{W/G}$	ppLFEr vs. SPARC	MAD	0.75	0.57	0.84	1.08	1.48	1.53	5.78	1.10
		MD	0.74	-0.09	-0.15	0.38	0.87	1.45	5.76	0.36
	COSMOtherm vs. SPARC	MAD	0.51	0.86	1.61	2.31	3.78	4.34	4.55	2.23
		MD	0.48	-0.59	-1.44	-2.18	-3.74	-4.04	-4.36	-2.06
	COSMOtherm vs. ppLFEr	MAD	0.40	1.16	1.64	2.63	4.62	5.55	10.09	2.64
		MD	-0.26	-0.50	-1.29	-2.56	-4.61	-5.50	-10.05	-2.42

200 Dependence of Partitioning Coefficients on Attributes of the Compounds

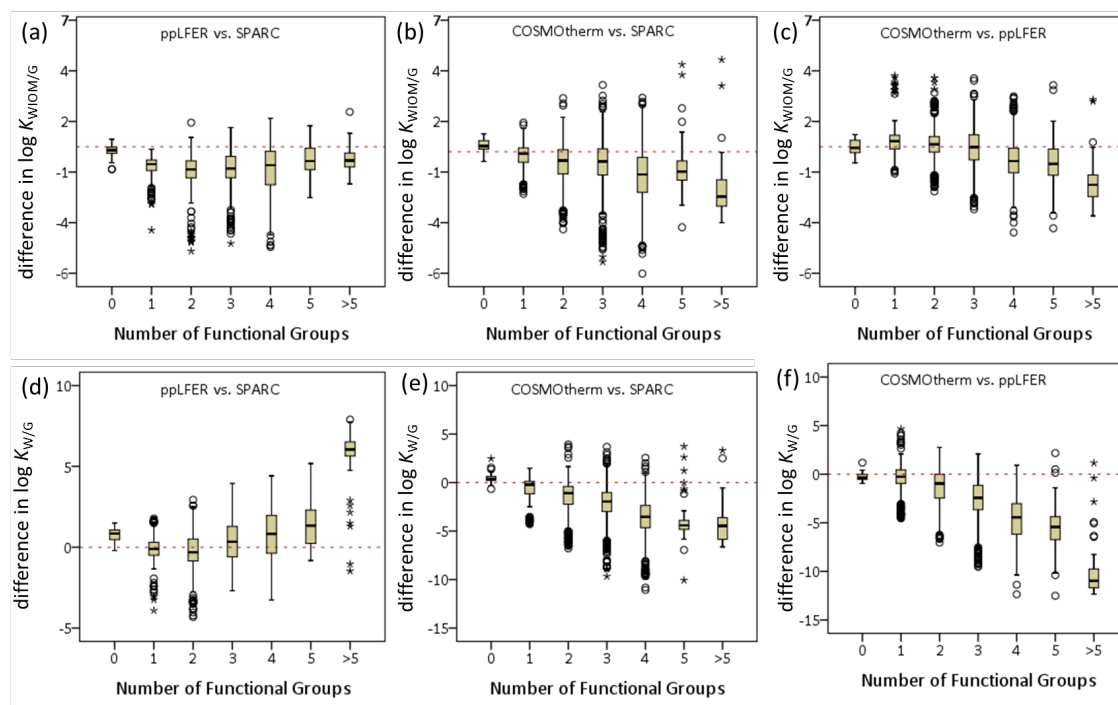
201 The equilibrium partitioning coefficients depend on molecular attributes. Here we explored this
 202 dependency on the number of functional groups, molecular mass, generation of oxidation,
 203 number of oxygens and O:C ratio.

204 Previous work observed that discrepancies between vapor pressure predictions by different
 205 methods increased with the number of functional groups in atmospherically relevant organic



206 compounds (Valorso et al., 2011; Barley and McFiggans, 2010). For instance, the MAD between
207 different vapor pressure predictions increased from 0.47 to 3.6 log units when the number of
208 functional groups in the molecules increased from one to more than three (Valorso et al., 2011).
209 In order to explore if the partitioning coefficients predicted with SPARC, ABSOLV/ppLFER and
210 COSMOtherm show the same dependence on the number of functional groups, we counted the
211 number of hydroxyl (ROH), aldehyde (RCHO), ketone (RCOR'), carboxylic acid (RCOOH), ester
212 (RCOOR'), ether (ROR'), peracid (RCOOOH), peroxide (ROOH, ROOR'), nitrate (NO₃), peroxyacyl
213 nitrate (PAN), nitro (NO₂) groups, halogen (Cl, Br), and sulphur (S) in the 3414 molecules. About
214 two thirds (2243) of the compounds contain two or three functional groups (Table 1). 736
215 compounds contain more than three functional groups and the rest contains just one or no
216 functional group. In Figure 1 the compounds are colored according to the number of functional
217 groups in a molecule and Table 1 lists the MAD and MD between predictions based on the
218 number of functional groups. The predicted partitioning coefficients (both $K_{WIO/M/G}$ and $K_{W/G}$)
219 generally increase with the number of functional groups (Figure 1 and Figure S1). Compounds
220 with no functional groups are the precursor compounds, which generally have a smaller
221 discrepancy among different prediction methods.

222 The boxplots in Figure 2 show the difference in SPARC, ABSOLV/ppLFER and COSMOtherm
223 predictions for compounds having different number of functional groups. The mean absolute
224 difference in predicted log $K_{WIO/M/G}$ is almost always smaller than one log unit for compounds
225 with up to seven functional groups (Table 1). There is a slightly larger discrepancy in the
226 predicted log $K_{WIO/M/G}$ values for compounds with more than three functional groups. The
227 agreement among different methods does not deteriorate as much with increasing number of
228 functional groups as that among vapor pressure predictions. The largest MADs of 1.72 and 2.11
229 between COSMOtherm and ABSOLV/ppLFER, and between COSMOtherm and SPARC,
230 respectively, for compounds with >5 functional groups (Table 1) are still much lower than
231 discrepancies reported between different vapor pressure prediction methods (Valorso et al.,
232 2011).



233

234 **Figure 2** Boxplot of difference in SPARC, ABSOLV/ppLFER and COSMOtherm predictions for
235 compounds with different number of functional groups. The line inside each box shows
236 the median difference for $\log K_{WIOM/G}$ or $\log K_{W/G}$ for different categories of compounds.
237 The marker circle and star indicates possible outliers and extreme values, respectively.

238 Different from the predictions for $K_{WIOM/G}$, the discrepancy between COSMOtherm and SPARC
239 and between COSMOtherm and ABSOLV/ppLFER in the predicted $K_{W/G}$ increases significantly
240 with the number of functional groups (Figures 1 and 2), from less than one order of magnitude
241 for compounds with no functional groups to up to five orders of magnitude for compounds with
242 more than three functional groups (Table 1). In addition, the MD in Table 1 and Figure 2
243 indicate that the discrepancies are almost always in one specific direction, i.e. a lower value of
244 $K_{W/G}$ estimated by COSMOtherm. This is evidenced by the almost identical absolute values of
245 MAD and MD between COSMOtherm and ABSOLV/ppLFER and between COSMOtherm and
246 SPARC for compounds with more than three functional groups (Table 1). The uncertainty of the
247 SPARC, ABSOLV/ppLFER and COSMOtherm predictions of $K_{W/G}$ tends to increase with the



248 number of functional groups. Clearly, the reliability of $K_{W/G}$ estimates for multifunctional
249 compounds needs further assessment.

250 It is also possible to explore the dependence of the prediction discrepancy on other molecular
251 attributes, such as molecular mass (Figures S2 and S3), the number of oxygen in the molecule
252 (Figures S4 and S5), the O:C ratio (Figure S6), the number of oxidation steps a molecule has
253 undergone (oxidation generation, Figure S7), or the number of occurrences of a specific type of
254 functional group, e.g. hydroxyl, in a molecule (Figure S8). The prediction discrepancies become
255 larger with an increase in each of these parameters, especially for $K_{W/G}$. This is not surprising as
256 these molecular attributes all tend to be highly correlated, i.e. with each oxidation step a
257 molecule becomes more oxygenated, has a large molar mass, a larger number of oxygen, a
258 higher O:C ratio, and a larger number of functional groups.

259 Discussion

260 We believe there are primarily two factors that are contributing to errors in the prediction of
261 $K_{CP/G}$ for the SOA compounds. One is the lack of experimental data for compounds that are
262 similar to the SOA compounds, which implies that prediction methods relying on calibration
263 with experimental data are being used outside their applicability domain. The other is the
264 failure of some prediction methods to account for the various conformations that compounds
265 with multiple functional groups can undergo due to extensive intra-molecular interaction
266 (mostly internal hydrogen bonding, see Figure S9 for example). The two factors are related: in
267 some instances a prediction method cannot account for such conformations precisely because
268 the calibration data set does not contain compounds that undergo such intra-molecular
269 interactions.

270 SPARC relies to some extent on calibrations with empirical data. While the experimental data
271 underlying SPARC have not been disclosed, it is highly unlikely that they include multifunctional
272 compounds of atmospheric relevance (e.g. compounds containing multiple functional groups,
273 including peroxides, peroxy acids etc.), simply because such empirical data do not exist. It is
274 therefore safe to assume that many of the 3414 SOA compounds will fall outside of the domain



275 of applicability of SPARC. It is also likely that SPARC can only account for intra-molecular
276 interactions and conformations to a limited extent, if at all.

277 In the case of ppLFER, there are actually two predictions that rely on calibration with empirical
278 data, the prediction of solute descriptors and the prediction of $K_{CP/G}$. The solute descriptors are
279 predicted with ABSOLV, because experimentally measured descriptors are unavailable for
280 multifunctional atmospheric oxidation products. ABSOLV relies on a group contribution
281 approach (Platts et al., 1999) complemented by some other, undisclosed procedures that make
282 use of experimental partition coefficients between various phases (ACD/Labs, 2016). Again,
283 those experimental data do not comprise compounds structurally similar to the multifunctional
284 atmospheric oxidation products considered here. As a group contribution method, which adds
285 up the contributions of different functional groups to a compound's property, ABSOLV
286 therefore cannot, or only to a limited extent, consider the interactions between different
287 functional groups in a molecule.

288 Ideally, when supplied with well-characterized solute descriptors, ppLFERs should be able to
289 consider the influence of both intra-molecular interactions and the interactions a molecule has
290 with its surroundings, i.e. the involved partitioning phases. Even if a molecule has different
291 conformations in different phases, i.e. if the solute descriptors for a compound are phase
292 dependent, it is possible to derive well-calibrated "average" descriptors to use in a ppLFER
293 (Niederer and Goss, 2008). However ABSOLV cannot correctly predict such "average"
294 descriptors and our ppLFER predictions therefore cannot account for the influence of
295 conformations.

296 In the case of the actual ppLFER prediction of $K_{W/G}$ and $K_{WIO/M/G}$, the empirical calibration
297 datasets are public (Goss, 2006; Arp et al., 2008) and do not comprise compounds that are
298 representative of the 3414 SOA compounds in terms of the number of functional groups per
299 molecule or the range of K -values. For instance, the log $K_{W/G}$ of the 217 compounds Goss (2006)
300 used for the development of a ppLFER ranged from -2.4 to 7.4, i.e. the highest $K_{W/G}$ predicted
301 here is almost 14 orders of magnitude higher than the highest $K_{W/G}$ included in the calibration.
302 Similarly, Arp and Goss (2009) developed the ppLFERs for atmospheric aerosol from an



303 empirical dataset of 50~59 chemicals, whose $\log K_{W/IO/M/G}$ ranged from approximately 2 to 7. The
304 highest $K_{W/IO/M/G}$ predicted here is eight orders of magnitude higher. Predictions for compounds
305 outside of the calibration domain may introduce large errors and the high $K_{W/G}$ and $K_{W/IO/M/G}$
306 values estimated by ppLFEr can thus be expected to be highly uncertain. Overall, however, we
307 expect the uncertainty of the ABSOLV-predicted solute descriptors to be larger than the
308 uncertainty introduced by the ppLFEr equation, especially for the relatively well-calibrated
309 water/gas phase partition system.

310 In contrast to the other methods, COSMOtherm relies only in a very fundamental way on some
311 empirical calibrations (and these calibrations are not specific for specific compound classes or
312 partition systems) and it considers intra-molecular interactions and the different conformations
313 of a molecule. As such, COSMOtherm is not constrained by the limitations the other methods
314 face, namely the lack of suitable calibration data, which necessitates extreme extrapolations
315 and predictions beyond the applicability domain, and the failure to account for the effect of
316 intra-molecular interactions and conformations on the interactions with condensed phases.

317 Because intra-molecular interactions are likely to reduce the potential of a compound to
318 interact with condensed phases (i.e. the organic and aqueous phase), ignoring them can be
319 expected to lead to overestimated partitioning coefficients $K_{CP/G}$ and to underestimated vapor
320 pressures (P_L). This is consistent with COSMOtherm-predicted $K_{W/IO/M/G}$ and $K_{W/G}$ -values for
321 multifunctional compounds that are lower than the SPARC and ABSOLV/ppLFEr predictions (i.e.
322 $MD < 0$ in Table 1), because the latter do not account for the influence of intra-molecular
323 interactions. Kurtén et al. (2016) similarly found that COSMOtherm-predicted saturation vapor
324 pressures for most of the more highly oxidized monomers were significantly higher (up to 8
325 orders of magnitude) than those predicted by group-contribution methods. The wider range on
326 the higher end of the $\log C^*$ values estimated by Hodzic et al. (2014) is possibly due to the large
327 uncertainties associated with vapor pressure estimation (likely underestimation) for low volatile
328 compounds. Valorso et al. (2011) also found group contribution methods to underestimate the
329 saturation vapor pressure of multifunctional species.



330 Compared to $K_{\text{WIOM/G}}$, P_L and C^* , ignoring intra-molecular interaction is likely even more
331 problematic in the case of $K_{\text{W/G}}$ prediction. Intra-molecular interactions mostly affect the ability
332 of the molecule to undergo H-bonding with solvent molecules. The system constants describing
333 H-bond interactions (a and b) are larger in the ppLFER equations for $K_{\text{W/G}}$ than in the one for
334 $K_{\text{WIOM/G}}$ (Arp et al., 2008; Goss, 2006), indicating a stronger effect of H-bonds on water/gas
335 partitioning than WIOM/gas partitioning. This likely is the reason why the COSMOtherm-
336 predicted $K_{\text{W/G}}$ are so much lower than the $K_{\text{W/G}}$ predicted by the other two methods, whereas
337 the difference is much smaller for the $K_{\text{WIOM/G}}$ (Table 1). It likely also explains why the
338 discrepancies among the predicted $K_{\text{W/G}}$ increase with the number of functional groups. It is
339 more difficult to predict $K_{\text{W/G}}$ than $K_{\text{WIOM/G}}$, because the free energy cost of cavity formation in
340 water is influenced more strongly by H-bonding and therefore much more variable than in
341 WIOM. Certainly, the activity coefficient in water (γ_{W}) is much more variable than the activity
342 coefficient in WIOM (γ_{WIOM}) for the investigated substances. $\log \gamma_{\text{WIOM}}$ predicted by
343 COSMOtherm at 15 °C varies from -3.8 to 1.8 (with an average of 0.04, indicating a γ_{WIOM} close
344 to unity, and a standard deviation of 0.5, 94 % of the compounds have a $\log \gamma_{\text{WIOM}}$ between -1
345 and 1), whereas γ_{W} ranges from -2.3 to 8.9 (with an average of 2.7 and a standard deviation of
346 1.4) (Supporting information Excel spreadsheet and Figure S10).

347 In the absence of experimental data for multi-functional SOA compounds, we do not know
348 whether COSMOtherm-predicted $K_{\text{W/G}}$ and $K_{\text{WIOM/G}}$ values are any better than the other
349 predictions. For example, two earlier studies suggested that COSMOtherm might be
350 overestimating vapor pressures of multi-functional oxygen-containing compounds (Kurtén et al.,
351 2016; Schröder et al., 2016). However, we can infer that the:

352 - fact that COSMOtherm on the one hand and ABSOLV/ppLFERs and SPARC on the other hand
353 predict $K_{\text{WIOM/G}}$ that are on average within one order of magnitude for all studied
354 compounds, including highly oxygenated multifunctional organic compounds, lends
355 credibility to all three predictions and suggests that partly ignoring intra-molecular
356 interactions and extrapolating beyond the applicability domain incurs only limited errors in
357 the $K_{\text{WIOM/G}}$ prediction of ABSOLV/ppLFERs and SPARC. In addition, COSMOtherm and SPARC



358 use a single surrogate molecule to represent the WIOM phase, while ppLFERs were
359 calibrated from atmospheric aerosols. The agreement among different methods suggests
360 that the surrogate suitably represents the solvation properties of organic aerosol.
361 - generally better agreement between $K_{W/G}$ values predicted by ABSOLV/ppLFER and SPARC
362 (Figure 1 (d)) should not be seen as an indication that these methods are better at
363 predicting $K_{W/G}$. In fact, the lower $K_{W/G}$ values predicted by COSMOtherm have a higher
364 chance of being correct than the $K_{W/G}$ values predicted by ABSOLV/ppLFER and SPARC.

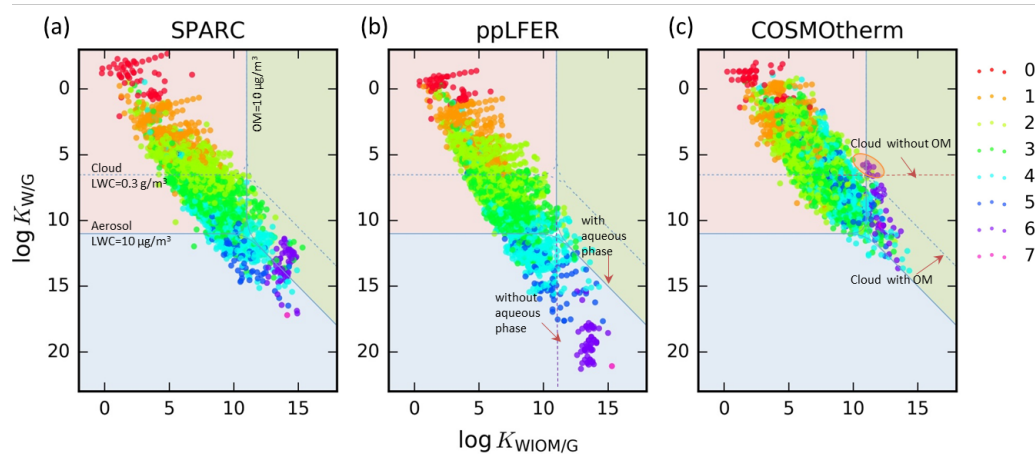
365 While ABSOLV/ppLFERs, SPARC and the group contributions methods currently used in the
366 atmospheric chemistry community are much more easily implemented for the large number of
367 compounds implicated in SOA formation, the current study demonstrates that the expertise
368 and time required to perform quantum-chemical calculations for atmospherically relevant
369 molecules should constitute but a minor impediment to a wider adoption of COSMOtherm
370 predictions. Here, we are not only compiling all the predictions we have made in the supporting
371 information file, we are also making available the cosmo-files (see Data Availability for details),
372 whose generation is the major time and CPU-demanding step in the use of COSMOtherm.

373 **Atmospheric Implications**

374 The phase distribution of an organic compound in the atmosphere depends on its partitioning
375 coefficients. The two-dimensional partitioning space defined by $\log K_{W/G}$ and $\log K_{WIOM/G}$
376 introduced recently (Wania et al., 2015) is used here to illustrate the difference in the
377 equilibrium phase distribution of these compounds in the atmosphere that arises from using
378 partitioning coefficients estimated by different methods (Figure 3). A detailed description of
379 partitioning space has been provided by Wania et al. (2015), a brief explanation is given in the
380 supporting information (Figure S11). Briefly, the blue solid lines between the differently colored
381 fields indicate partitioning property combinations that lead to equal distributions between two
382 phases in a phase-separated aerosol scenario, with a liquid water content (LWC) of $10 \mu\text{g}/\text{m}^3$
383 and organic matter loading (OM) of $10 \mu\text{g}/\text{m}^3$. The purple dashed line in Figure 3 (b) shows an
384 aerosol scenario without an aqueous phase (see Figure S11 (c) for detail). The blue dotted lines
385 represent a cloud scenario where LWC is $0.3 \text{ g}/\text{m}^3$ and OM is either $10 \mu\text{g}/\text{m}^3$ or non-existent



386 because all of the OM is dissolved in the aqueous phase (illustrated by the red dashed lines in
387 Figure 3 (c), see also Figure S11 (d)). Compounds are located in the partitioning space based on
388 their estimated partitioning coefficients ($K_{W/OM/G}$ and $K_{W/G}$). Compounds on the boundary lines
389 have 50 % in either of the two phases on both sides of the boundary and are thus most
390 sensitive to uncertain partitioning properties. On the other hand, for substances that fall far
391 from the boundary lines indicating a phase transition (e.g. volatile compounds with two or less
392 functional groups), even relatively large uncertainties in the partitioning coefficients could be
393 tolerated, because they are inconsequential.



394
395 **Figure 3** Partitioning space plot, showing in pink, blue and green the combinations of partitioning
396 properties that lead to dominant equilibrium partitioning to the gas, aqueous, and
397 WIOM phases, respectively. The blue solid and dotted lines are boundaries for an
398 aerosol scenario (LWC 10 $\mu\text{g}/\text{m}^3$, 10 $\mu\text{g}/\text{m}^3$ OM) and a cloud scenario (LWC 0.3 g/m^3 , 10
399 $\mu\text{g}/\text{m}^3$ OM), respectively. The vertical purple dashed lines in Figure 3 (b) shows an
400 aerosol scenario without an aqueous phase (LWC 0 $\mu\text{g}/\text{m}^3$, 10 $\mu\text{g}/\text{m}^3$ OM). The
401 horizontal red dashed lines in Figure 3 (c) represent a cloud scenario where LWC is 0.3
402 g/m^3 and OM 0 $\mu\text{g}/\text{m}^3$. The differently colored dots indicate the number of functional
403 groups in the molecules.

404 When plotted in the chemical partition space, the 3414 chemicals occupy more or less the same
405 region as the much smaller set of SOA compounds investigated earlier (Wania et al., 2015).
406 When using predictions by COSMOtherm the SOA compounds cover a relatively smaller region



407 as compared to ABSOLV/ppLFER and SPARC. With increasing number of functional groups
408 (Figure 3) or molecular weight (Figure S12), an increasing fraction of these compounds
409 partitions into the condensed phases, i.e. WIOM or water. In general, compounds with water or
410 WIOM as the dominant phase usually are multifunctional, i.e. contain more than two functional
411 groups. According to Figure S12, compounds with predominant partitioning into WIOM usually
412 have a molar mass in excess of 200 g/mol, while some compounds with molar mass less than
413 200 g/mol prefer the aqueous phase. Other than the water content and WIOM loadings
414 illustrated in Figure 3, in reality a compound's atmospheric phase distribution depends on other
415 factors such as the organic matter composition, salt content, pH, and temperature (Wania et
416 al., 2015; Wang et al., 2015).

417 Comparing the different panels of Figure 3 reveals that the atmospheric equilibrium phase
418 distribution of SOA compounds can be very different depending on which methods is used for
419 partitioning coefficient estimation. The difference is most striking when comparing the
420 placement of highly functionalized compounds (with more than 3 functional groups) based on
421 ABSOLV/ppLFER and COSMOtherm predictions. The large $K_{W/G}$ values estimated by
422 ABSOLV/ppLFERs lead to these compounds having a high affinity for aqueous aerosol. In
423 contrast, predictions by COSMOtherm suggest that only very few of them (and not even the
424 ones with the highest number of functional groups) prefer the aqueous aerosol phase; instead
425 most of them have either gas or WIOM as the dominant phase. SPARC predicts a slightly larger
426 preference of highly functionalized compounds for the aqueous phase than COSMOtherm.

427 In a cloud scenario with a much higher LWC (shown by the blue dotted boundary lines in Figure
428 3), the choice of $K_{W/G}$ prediction method also matters. Whereas with ABSOLV/ppLFER and
429 SPARC most of the highly functionalized compounds (i.e. 96 % or 97 % of the 736 compounds
430 with >3 functional groups) partitions into aqueous phase, only two-thirds (64 %) do so when the
431 $K_{W/G}$ s predicted by COSMOtherm are used. Further, only COSMOtherm predicts that some of
432 the SOA compounds (circled in Figure 3(c)) would prefer to form a separate WIOM phase rather
433 than dissolve in the bulk aqueous phase.



434 Table 2 summarizes the number and percentage of compounds that have dominant partitioning
 435 (at least 50 %) into different phases, which shows the impact of using different prediction
 436 techniques on phase distribution calculations in different atmospheric scenarios. In a para-
 437 meterisation of SOA formation that includes an aqueous aerosol phase, use of $K_{W/G}$ predicted
 438 by ABSOLV/ppLFRs (and probably also the commonly employed group contribution methods)
 439 would lead to much higher SOA mass than use of $K_{W/G}$ predicted by COSMOtherm. For instance,
 440 10 % and 17 % of the compounds predominantly partition into the aqueous phase when
 441 predictions by SPARC and ABSOLV/ppLFR are used, in contrast to only 14 compounds (less
 442 than 1 %) with COSMOtherm predictions (Table 2 scenario (a)). A large difference also occurs in
 443 the cloud scenarios (Table 2 scenarios (b) and (d)), where SPARC and ABSOLV/ppLFR predict
 444 twice as many compounds partitioning into the aqueous phase than COSMOtherm. Incidentally,
 445 in a parameterization of SOA formation that does not account for an aqueous aerosol phase
 446 (the scenario in Figure S11 (c) and Table 2 (c)), the impact of the choice of partitioning
 447 prediction method is much smaller. The number of compounds on the right side of the purple
 448 dashed boundary in Figure 3 (b) does not vary substantially with different predictions.

449 **Table 2** Percentage and number of compounds with at least 50 % in gas, water or WIOM phase
 450 under different aerosol and cloud scenarios predicted with SPARC, ABSOLV/ppLFR and
 451 COSMOtherm. The four scenarios (a-d) correspond to the scenarios in Figure S11 (a-d) in
 452 Supporting information.

aerosol scenarios	(a) (LWC=10 $\mu\text{g}/\text{m}^3$, OM=10 $\mu\text{g}/\text{m}^3$)			(c) without water phase (LWC=0 $\mu\text{g}/\text{m}^3$, OM=10 $\mu\text{g}/\text{m}^3$)	
	$\Phi_G > 50\%$ ^a	$\Phi_W > 50\%$ ^a	$\Phi_{\text{WIOM}} > 50\%$ ^a	$\Phi_G > 50\%$	$\Phi_{\text{WIOM}} > 50\%$
SPARC	85 % (2892) ^b	10 % (352)	4 % (134)	92 % (3132)	8 % (282)
ABSOLV/ppLFR	82 % (2804)	17 % (570)	1 % (25)	96 % (3267)	4 % (141)
COSMOtherm	96 % (3268)	0 % (14)	3 % (119)	96 % (3282)	4 % (131)
cloud scenarios	(b) (LWC=0.3 g/m^3 , OM=10 $\mu\text{g}/\text{m}^3$)			(d) without WIOM phase (LWC=0.3 g/m^3 , OM=0 $\mu\text{g}/\text{m}^3$)	
	$\Phi_G > 50\%$	$\Phi_W > 50\%$	$\Phi_{\text{WIOM}} > 50\%$	$\Phi_G > 50\%$	$\Phi_W > 50\%$
SPARC	36 % (1242)	64 % (2168)	0 % (0)	36 % (1242)	64 % (2172)
ABSOLV/ppLFR	35 % (1201)	65 % (2211)	0 % (0)	35 % (1203)	65 % (2211)
COSMOtherm	66 % (2258)	33 % (1137)	0 % (9)	66 % (2267)	34 % (1147)

453 ^a Φ_G , Φ_W and Φ_{WIOM} represent for fractions of compounds in gas phase, water phase and WIOM phase, respectively.

454 ^b number in brackets are number of compounds



455 **Conclusions**

456 For compounds implicated in SOA formation, the prediction of $K_{W/G}$ is much more uncertain
457 than the prediction of $K_{WIOM/G}$. This is true even if we consider that $K_{WIOM/G}$ will vary somewhat
458 depending on the composition of the WIOM (Wang et al., 2015). In particular, the methods
459 currently used for $K_{W/G}$ prediction of these substances have the potential to greatly
460 overestimate $K_{W/G}$. This uncertainty is consequential, as the predicted equilibrium phase
461 distribution in the atmosphere, and therefore also the predicted aerosol yield, is very sensitive
462 to the predicted values of $K_{W/G}$: depending on the method used for prediction, the aqueous
463 phase is either very important for SOA formation from the studied set of compounds or hardly
464 at all. Isaacman-VanWertz et al. (2016) recently found the estimated phase distribution of 2-
465 methylerythritol, an isoprene oxidation product (in Figure S6), highly dependent on the chosen
466 method for predicting $K_{W/G}$. Here we show that this is a general issue potentially affecting a
467 very large number of SOA compounds. In order to identify reliable prediction methods, it will be
468 necessary to experimentally determine the phase distribution of highly functionalized,
469 atmospherically relevant substances, whereby the focus should be on establishing their
470 partitioning into aqueous aerosol.

471 **Data Availability**

472 COSMO files for the 3414 organic compounds can be accessed by contacting the corresponding
473 author.

474 **Supporting Information**

475 The supporting information contains figures and text mentioned in the paper, including detailed
476 information on the organic compounds, e.g. SMILES, molecular formula, molecular weight,
477 functional groups, O:C ratios, predicted K -values, ABSOLV predicted solute descriptors,
478 COSMOtherm predicted vapor pressures and activity coefficients in WIOM and water.



479 **Acknowledgement**

480 We acknowledge funding from Natural Sciences and Engineering Research Council of Canada.
481 Computations for the COSMO files in this study were performed on the General Purpose Cluster
482 (GPC) supercomputer at the SciNet HPC Consortium. SciNet is funded by: the Canada
483 Foundation for Innovation under the auspices of Compute Canada; the Government of Ontario;
484 Ontario Research Fund - Research Excellence; and the University of Toronto.

485 **References**

- 486 ACD/Labs: Advanced Chemistry Development. Data sheet: Absolv prediction module. Toronto (Canada).
487 [cited 2016 December 2]. Available
488 from: http://www.acdlabs.com/download/docs/datasheets/datasheet_absolv.pdf, 2016.
- 489 Arp, H. P. H., Schwarzenbach, R. P., and Goss, K. U.: Ambient gas/particle partitioning. 2: The influence of
490 particle source and temperature on sorption to dry terrestrial aerosols, *Environmental Science &*
491 *Technology*, 42, 5951-5957, 10.1021/es703096p, 2008.
- 492 Arp, H. P. H., and Goss, K. U.: Ambient Gas/Particle Partitioning. 3. Estimating Partition Coefficients of
493 Apolar, Polar, and Ionizable Organic Compounds by Their Molecular Structure, *Environmental Science &*
494 *Technology*, 43, 1923-1929, 10.1021/es8025165, 2009.
- 495 Barley, M. H., and McFiggans, G.: The critical assessment of vapour pressure estimation methods for use
496 in modelling the formation of atmospheric organic aerosol, *Atmospheric Chemistry and Physics*, 10, 749-
497 767, 10.5194/acp-10-749-2010, 2010.
- 498 Endo, S., Pfennigsdorff, A., and Goss, K. U.: Salting-out effect in aqueous NaCl solutions: trends with size
499 and polarity of solute molecules, *Environmental Science & Technology*, 46, 1496-1503,
500 10.1021/es203183z, 2012.
- 501 Goss, K.-U.: Prediction of the Temperature Dependency of Henry's Law Constant using Poly-Parameter
502 Linear Free Energy Relationships, *Chemosphere*, 64, 1369-1374, 2006.
- 503 Hilal, S. H., Karickhoff, S. W., and Carreira, L. A.: Prediction of the solubility, activity coefficient and
504 liquid/liquid partition coefficient of organic compounds, *Qsar & Combinatorial Science*, 23, 709-720,
505 2004.
- 506 Hilal, S. H., Ayyampalayam, S. N., and Carreira, L. A.: Air-Liquid Partition Coefficient for a Diverse Set of
507 Organic Compounds: Henry's Law Constant in Water and Hexadecane, *Environmental Science &*
508 *Technology*, 42, 9231-9236, doi:10.1021/es8005783, 2008.
- 509 Hodzic, A., Aumont, B., Knote, C., Lee-Taylor, J., Madronich, S., and Tyndall, G.: Volatility dependence of
510 Henry's law constants of condensable organics: Application to estimate depositional loss of secondary
511 organic aerosols, *Geophysical Research Letters*, 41, 4795-4804, 10.1002/2014gl060649, 2014.
- 512 Ip, H. S. S., Huang, X. H. H., and Yu, J. Z.: Effective Henry's law constants of glyoxal, glyoxylic acid, and
513 glycolic acid, *Geophysical Research Letters*, 36, 10.1029/2008gl036212, 2009.



- 514 Isaacman-VanWertz, G., Yee, L. D., Kreisberg, N. M., Wernis, R., Moss, J. A., Hering, S. V., de Sá, S. S.,
515 Martin, S. T., Alexander, M. L., Palm, B. B., Hu, W., Campuzano-Jost, P., Day, D. A., Jimenez, J. L., Riva, M.,
516 Surratt, J. D., Viegas, J., Manzi, A., Edgerton, E., Baumann, K., Souza, R., Artaxo, P., and Goldstein, A. H.:
517 Ambient Gas-Particle Partitioning of Tracers for Biogenic Oxidation, *Environmental Science &*
518 *Technology*, 50, 9952-9962, 10.1021/acs.est.6b01674, 2016.
- 519 Kalberer, M., Paulsen, D., Sax, M., Steinbacher, M., Dommen, J., Prevot, A. S. H., Fisseha, R., Weingartner,
520 E., Frankevich, V., Zenobi, R., and Baltensperger, U.: Identification of polymers as major components of
521 atmospheric organic aerosols, *Science*, 303, 1659-1662, 10.1126/science.1092185, 2004.
- 522 Klamt, A., and Eckert, F.: COSMO-RS: a novel and efficient method for the a priori prediction of
523 thermophysical data of liquids, *Fluid Phase Equilibria*, 172, 43-72, 2000.
- 524 Klamt, A.: *From Quantum Chemistry to Fluid Phase Thermodynamics and Drug Design*, Elsevier,
525 Amsterdam, 2005.
- 526 Kroll, J. H., Donahue, N. M., Jimenez, J. L., Kessler, S. H., Canagaratna, M. R., Wilson, K. R., Altieri, K. E.,
527 Mazzoleni, L. R., Wozniak, A. S., Bluhm, H., Mysak, E. R., Smith, J. D., Kolb, C. E., and Worsnop, D. R.:
528 Carbon oxidation state as a metric for describing the chemistry of atmospheric organic aerosol, *Nature*
529 *Chemistry*, 3, 133-139,
530 <http://www.nature.com/nchem/journal/v3/n2/abs/nchem.948.html#supplementary-information>, 2011.
- 531 Kurtén, T., Tiusanen, K., Roldin, P., Rissanen, M., Luy, J.-N., Boy, M., Ehn, M., and Donahue, N.: α -Pinene
532 autoxidation products may not have extremely low saturation vapor pressures despite high O:C ratios,
533 *The Journal of Physical Chemistry A*, 120, 2569-2582, 10.1021/acs.jpca.6b02196, 2016.
- 534 Loken, C., Gruner, D., Groer, L., Peltier, R., Bunn, N., Craig, M., Henriques, T., Dempsey, J., Yu, C.-H., Chen,
535 J., Dursi, L. J., Chong, J., Northrup, S., Pinto, J., Knecht, N., and Van Zon, R.: SciNet: Lessons Learned from
536 Building a Power-efficient Top-20 System and Data Centre, *Journal of Physics: Conference Series*, 256,
537 012026, 2010.
- 538 McFiggans, G., Topping, D. O., and Barley, M. H.: The sensitivity of secondary organic aerosol component
539 partitioning to the predictions of component properties - Part 1: A systematic evaluation of some
540 available estimation techniques, *Atmospheric Chemistry and Physics*, 10, 10255-10272, 10.5194/acp-10-
541 10255-2010, 2010.
- 542 Mouchel-Vallon, C., Bräuer, P., Camredon, M., Valorso, R., Madronich, S., Herrmann, H., and Aumont, B.:
543 Explicit modeling of volatile organic compounds partitioning in the atmospheric aqueous phase, *Atmos.*
544 *Chem. Phys.*, 13, 1023-1037, 10.5194/acp-13-1023-2013, 2013.
- 545 Niederer, C., and Goss, K.-U.: Effect of ortho-chlorine substitution on the partition behavior of
546 chlorophenols, *Chemosphere*, 71, 697-702, 2008.
- 547 Platts, J. A., Butina, D., Abraham, M. H., and Hersey, A.: Estimation of Molecular Linear Free Energy
548 Relation Descriptors Using a Group Contribution Approach, *J. Chem. Inf. Comput. Sci.*, 39, 835-845, 1999.
- 549 Raventos-Duran, T., Camredon, M., Valorso, R., Mouchel-Vallon, C., and Aumont, B.: Structure-activity
550 relationships to estimate the effective Henry's law constants of organics of atmospheric interest,
551 *Atmospheric Chemistry and Physics*, 10, 7643-7654, 10.5194/acp-10-7643-2010, 2010.
- 552 Sander, R.: *Compilation of Henry's law constants (version 4.0) for water as solvent*, *Atmospheric*
553 *Chemistry and Physics*, 15, 4399-4981, 10.5194/acp-15-4399-2015, 2015.



- 554 Schröder, B., Fulem, M., and Martins, M. A. R.: Vapor pressure predictions of multi-functional oxygen-
555 containing organic compounds with COSMO-RS, *Atmospheric Environment*, 133, 135-144,
556 <http://dx.doi.org/10.1016/j.atmosenv.2016.03.036>, 2016.
- 557 US EPA: Estimation Programs Interface Suite™ for Microsoft® Windows, v 4.11 or insert version used].
558 United States Environmental Protection Agency, Washington, DC, USA., 2012.
- 559 Valorso, R., Aumont, B., Camredon, M., Raventos-Duran, T., Mouchel-Vallon, C., Ng, N. L., Seinfeld, J. H.,
560 Lee-Taylor, J., and Madronich, S.: Explicit modelling of SOA formation from alpha-pinene photooxidation:
561 sensitivity to vapour pressure estimation, *Atmospheric Chemistry and Physics*, 11, 6895-6910,
562 10.5194/acp-11-6895-2011, 2011.
- 563 Wang, C., Lei, Y. D., Endo, S., and Wania, F.: Measuring and modeling the salting-out effect in
564 ammonium sulfate solutions, *Environmental Science & Technology*, 48, 13238-13245,
565 10.1021/es5035602, 2014.
- 566 Wang, C., Goss, K.-U., Lei, Y. D., Abbatt, J. P. D., and Wania, F.: Calculating equilibrium phase distribution
567 during the formation of secondary organic aerosol using COSMOtherm, *Environmental Science &
568 Technology*, 49, 8585-8594, 10.1021/acs.est.5b01584, 2015.
- 569 Wang, C., Lei, Y. D., and Wania, F.: Effect of Sodium Sulfate, Ammonium Chloride, Ammonium Nitrate,
570 and Salt Mixtures on Aqueous Phase Partitioning of Organic Compounds, *Environmental Science &
571 Technology*, 50, 12742-12749, 10.1021/acs.est.6b03525, 2016.
- 572 Wania, F., Lei, Y. D., Wang, C., Abbatt, J. P. D., and Goss, K. U.: Novel methods for predicting gas-particle
573 partitioning during the formation of secondary organic aerosol, *Atmospheric Chemistry and Physics*, 14,
574 13189-13204, 10.5194/acp-14-13189-2014, 2014.
- 575 Wania, F., Lei, Y. D., Wang, C., Abbatt, J. P. D., and Goss, K. U.: Using the chemical equilibrium
576 partitioning space to explore factors influencing the phase distribution of compounds involved in
577 secondary organic aerosol formation, *Atmospheric Chemistry and Physics*, 15, 3395-3412, 10.5194/acp-
578 15-3395-2015, 2015.
- 579 Waxman, E. M., Elm, J., Kurtén, T., Mikkelsen, K. V., Ziemann, P. J., and Volkamer, R.: Glyoxal and
580 methylglyoxal setschenow salting constants in sulfate, nitrate, and chloride solutions: measurements
581 and Gibbs energies, *Environmental Science & Technology*, 49, 11500-11508, 10.1021/acs.est.5b02782,
582 2015.